

**DELINEATING THE MAJOR KREEP-BEARING TERRANES ON THE MOON WITH GLOBAL MEASUREMENTS OF ABSOLUTE THORIUM ABUNDANCES.** D. J. Lawrence<sup>1</sup>, W. C. Feldman<sup>1</sup>, B. L. Barraclough<sup>1</sup>, A. B. Binder<sup>2</sup>, R. C. Elphic<sup>1</sup>, S. Maurice<sup>3</sup>, M. C. Miller<sup>4</sup> and T. H. Prettyman<sup>5</sup>, Los Alamos National Laboratory, Group NIS-1, MS D466, Los Alamos, NM 87545 (djlawrence@lanl.gov), <sup>2</sup>Lunar Research Institute, 1180 Sunrise Dr., Gilroy, CA 95020 USA, <sup>3</sup>Observatoire Midi-Pyrénées, Toulouse, FRANCE, <sup>4</sup>Lawrence Livermore National Laboratory, Livermore, CA 94551 USA, <sup>5</sup>Los Alamos National Laboratory, Group NIS-5, Los Alamos, NM 87545 USA.

**Introduction:** The Lunar Prospector (LP) Gamma-Ray Spectrometer (GRS) has been used to map the global composition of thorium on the lunar surface. Previous LP results of relative thorium abundances demonstrated that thorium is highly concentrated in and around the nearside western maria and less so in the South Pole Aitken (SPA) basin. Using new detector modeling results and a larger data set, we present here a global map of absolute thorium abundances on a 2° by 2° equal-area pixel scale. Because thorium is a tracer of KREEP-rich material, these data provide fundamental information regarding the locations and importance of terranes that are rich in KREEP bearing materials.

**Approach:** Thorium abundance measurements are obtained from the GRS data by measuring the counting rate of the 2.6 MeV line produced by the radioactive decay of thorium atoms. For this study, we have used counting rate data taken over 9-1/2 months from 16 Jan 1998 to 29 Oct 1998. Before these counting rates can be used, various corrections need to be made to the data as outlined in [1]. These include corrections for detector dead time, detector gain, galactic cosmic ray variations and detector response due to latitude variations. Since the publication of [1], we have also made corrections (on the order of ~5%) for variations of the Moon's solid angle as seen by the GRS. These solid angle variations arise because the spacecraft distance from the Moon varies from 80 to 120 km.

A rigorous determination of absolute thorium abundances requires a series of detector modeling and spectral fitting procedures to be carried out. However, because the 2.6 MeV thorium line has a large flux, has few competing  $\gamma$ -ray lines, and has large variations over the lunar surface, we can obtain an estimate of the absolute thorium abundance,  $A_{Th}$ , using the following relation:

$$C_{Th} = A_{Th} a \epsilon(2.6) F_{Th}. \quad (1)$$

Here,  $C_{Th}$  is the measured thorium counting rate per 32 seconds above background,  $a$  is the GRS area for  $\gamma$ -rays measured at the lunar equator (the area of the GRS bismuth-germanate crystal is 54 cm<sup>2</sup>),  $\epsilon(2.6)$  is the GRS detector efficiency at 2.6 MeV, and  $F_{Th}$  is the expected flux of thorium  $\gamma$ -rays per  $\mu\text{g/g}$  of thorium. In order for equation 1 to be valid, we have to make the

following assumptions: 1) the background counts under the thorium line are constant over the Moon; 2) the minimum counting rate in a given 2° by 2° equal area pixel is defined at the background counting rate, i.e. the pixel with the minimum counting rate is defined to have a thorium abundance of 0  $\mu\text{g/g}$ . The full-energy peak efficiency in equation 1 has recently been calculated for the LP GRS to be 0.4 counts per incident  $\gamma$ -ray at 2.6 MeV. The flux  $F_{Th}$  is taken from Reedy [2] to be 0.612  $\gamma/[\text{cm}^2 \cdot 32\text{s} \cdot (\mu\text{g/g})]$ .

**Results:** Figure 1 shows the map of absolute thorium abundances derived using equation 1. This map shows lunar nearside and farside orthographic projections centered on Mare Imbrium and the antipode to Mare Imbrium. Contours of the lunar albedo taken from Clementine data [3] are shown for latitude between 70° S and 70°N.

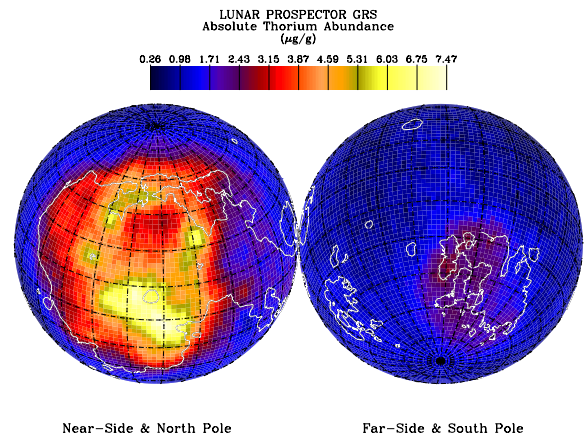


**Figure 1:** Map of absolute thorium abundances in  $\mu\text{g/g}$  for the lunar nearside and farside.

To check the validity of our assumptions, we have compared our results to measurements made using the Apollo GRS [4] for various Apollo and Luna landing sites as seen in figure 2. The LP measurements in figure 2 are the mean value abundances for the 2° by 2° pixel containing each landing site. The error bars show the standard deviation within each pixel and generally represent the systematic uncertainties of the data. These uncertainties are on the order of 6-8%. It is possible that there may be other systematic errors, but

we do not expect them to be greater than 15-20%.

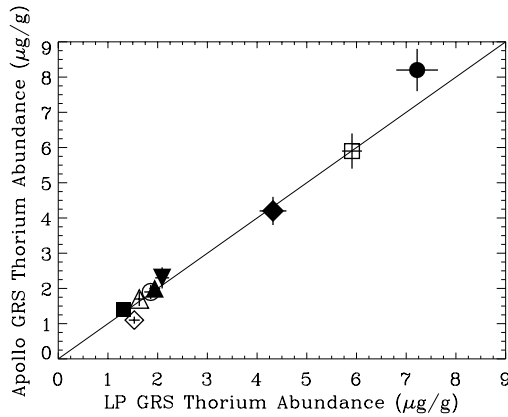


**Figure 2:** Comparison of the absolute thorium abundance measured by the LP GRS to the absolute thorium abundance measured by the Apollo 15 and 16 GRS for various Apollo and Luna landing sites. The symbols for the different landing sites are as follows: ▼–Apollo 11; ◻–Apollo 12; ●–Apollo 14; ◆–Apollo 15; ▲–Apollo 16; ○–Apollo 17; △–Luna 16; ◇–Luna 20; ■–Luna 24.

As seen, the comparison between the LP and Apollo GRS measurements is quite good. In fact, only two sites, Apollo 14 and Luna 20, have measurements that differ significantly from the slope 1 line (shown as the thick solid line). From this comparison, we believe these global measurements give a reasonably good representation of the absolute thorium abundance on the Moon.

**Regional Abundances:** With these measurements, we can make a survey of the degree to which various regions or terranes contain KREEP bearing minerals. Table 1 lists the mean abundances of various regions that can be delineated from figure 1.

The entire nearside high-thorium region, or “Great Lunar Hot Spot” [5], has a mean thorium abundance of 4.1 µg/g. Within this area, the highest thorium abundance region can be defined as the Copernicus/Fra Mauro region with a mean abundance of 6.2 µg/g. With this new 2° by 2° map, we can also delineate four other regions of high thorium abundance, namely: the Jura Mountains northwest of Mare Imbrium and south of Mare Frigoris (5.2 µg/g), the Aristarchus crater west of Mare Imbrium (5.3 µg/g), Aristillus crater east of Mare Imbrium (5.7 µg/g), and Archimedes crater southeast of Mare Imbrium (5.4 µg/g). Interestingly, the area within the nearside high-thorium region with the lowest thorium abundance is the center of Mare Imbrium. However, the local minimum of 2.9 µg/g is located not at the center of Mare Imbrium at 18°W,

33°N, but 9° north at 18°W and 42°N.

Region	Mean thorium abundance (µg/g)
“Great Lunar Hot Spot”	4.1
Copernicus/Fra Mauro	6.2
Jura Mountains	5.2
Aristarchus	5.3
Aristillus	5.7
Archimedes	5.4
Imbrium Basin	3.6
South Pole Aitken Basin	1.9
Lunar highlands (15°N-45°N -160°W-130°W)	0.6

**Table 1:** Mean thorium abundance for various lunar locations.

Apart from the high abundances of the nearside, the only other region of elevated thorium abundances is in the South Pole Aitken (SPA) basin. The SPA region, as defined from the Clementine topography data has an average thorium abundance of 1.9 µg/g. This contrasts to the eastern highlands region which has a low thorium abundance of 0.6 µg/g.

**References:** [1] Lawrence, D. J., et al. (1998) *Science*, **281**, 1484. [2] Reedy, R. C. (1978) *Proc. Lunar Planet. Sci. Conf.*, **9**, 2961. [3] Smith, D. E., et al., (1997) *J. Geophys. Res.*, **102** 1591; Lucey, P. G., et al. (1995) *Science*, **266**, 1855. [4] Metzger, A. E., in *Remote Geochemical Analysis: Elemental and Mineralogical Composition*, C. M. Pieters and P. A. J. Englert, Eds. (Cambridge Univ. Press, 1993), pp. 341-363. [5] term borrowed from R. L. Korotov et al. at the workshop *New Views of the Moon: Integrated Remotely Sensed, Geophysical, and Sample Datasets*, September 18-20, 1998, Houston, TX.